INVESTIGATION OF GOLD WIRE ATTACHMENT DURING LED ENCAPSULATION PROCESS USING COMPUTATIONAL FLUID DYNAMIC

By:

MOHAMMAD NOR FIKRI BIN SAHABARUDIN
(Matrix no.:137834)

UNIVERSITI SAINS MALAYSIA

2021

INVESTIGATION OF GOLD WIRE ATTACHMENT DURING LED ENCAPSULATION PROCESS USING COMPUTATIONAL FLUID DYNAMIC

By:

MOHAMMAD NOR FIKRI BIN SAHABARUDIN
(Matrix no.:137834)

Supervisor:

Dr. Mohd Sharizal Abdul Aziz

July 2021

This dissertation is submitted to
Universiti Sains Malaysia
As partial fulfilment of the requirement to graduate with honors degree in
BACHELOR OF ENGINEERING (MECHANICAL ENGINEERING)

School of Mechanical Engineering
Engineering Campus
University Sains Malaysia

ACKNOWLEDGEMENT

Foremost, I would like to express my gratitude to The Almighty Allah for the wisdom He bestowed upon me, giving me strength, peace of mind and good health in order to finish this research and manage to complete it within the planned time.
I would like to thank Assoc. Prof. Dr. Jamaluddin Abdullah, Dean of School of Mechanical Engineering, Universiti Sains Malaysia for giving me the opportunity to carry out this research.
Moreover, I would like to express my gratitude to my respectable supervisor, Dr. Mohd Sharizal Bin Abdul Aziz, lecturer School of Mechanical Engineering for his guidance and help throughout the whole project. It was honor to study under his guidance since he sincerely helps me sort out the confusion I am facing. I am thankful for all the contribution in stimulating suggestions and encouragement which helps me to carry out the research smoothly during the FYP period.
Next, throughout this research my family members have been the most ardent advocates. Their moral and financial support enabled me to fulfil the objective of this research and I believed without them this research will only be a dream.
Lastly, I would like to express my gratitude to all the lecturers and technical staffs in School of Mechanical Engineering, Universiti Sains Malaysia for sharing the knowledge and gave permission to use the equipment for me to complete this project.

TABLE OF CONTENTS

LIST OF TABLES

Page

LIST OF FIGURES

Page

LIST OF SYMBOLS

ρ	Density
t	Time
v	Velocity
p	Static pressure
μ	Viscosity
g_x	Gravitational acceleration

LIST OF ABBREVIATIONS

LED	Light Emitting Diode
CPI	Color Rendering Index
OLED	Organic Light Emitting Diode
PCB	Printed Circuit Board
EMC	Epoxy Molding Compound
VOF	Volume of Fluid
FSI	Fluid Structure Interaction
LID	Light Intensity Distribution
YBR	Yellow-Blue Ratio
CCT	Correlated Color Temperature
CFD	Computational Fluid Dynamic
IPS	Institut Pengajian Siswazah
USM	Universiti Sains Malaysia

LIST OF APPENDICES

ABSTRAK

Tujuan penyelidikan ini adalah untuk mengkaji kaedah enkapsulasi LED dan interaksi ikatan wayar emas dan EMC. Proses enkapsulasi penting kerana berfungsi sebagai lapisan perlindungan pertama LED. Seperti yang disebutkan dalam kajian sebelumnya, proses enkapsulasi memberikan kesan pada kualiti produk. Kecerahan dan warna cahaya yang dipancarkan akan dipengaruhi oleh struktur enkapsulan. Hasilnya, salah satu elemen yang dapat meningkatkan kualiti produk adalah EMC yang dipilih sebagai enkapsulan kerana ia menawarkan banyak kelebihan berbanding enkapsulan yang lain. Semasa proses enkapsulasi berlaku, faktor lain yang perlu dipertimbangkan adalah kadar halaju. Kadar halaju akan berbeza-beza dalam penyelidikan ini untuk melihat kesan tekanan terhadap ikatan wayar dan mengenal pasti isi padu cecair semasa proses enkapsulasi. Tekanan maksimum bergantung pada kadar halaju di mana peningkatan halaju, akan mengakibatkan penurunan tekanan.Halaju yang tinggi akan menghasilkan isipadu cecair yang rendah. Fluent ANSYS akan digunakan untuk melakukan proses enkapsulasi secara maya dengan menggunakan VOF untuk merangsang pengeluaran EMC. Satu eksperimen telah dijalankan untuk mengesahkan hasil teori dan hasil eksperimen.

ABSTRACT

The aim of this research is to investigate the LED encapsulation method and the interaction of gold wire bonding with EMC. The encapsulation process is important because it serves as the LED's first layer of protection. As noted in the preceding study, the encapsulating process has an impact on product quality. The brightness and colour of the light emitted will be affected by the encapsulant's structure. As a result, one the element that can increase the product quality is the EMC which is chosen as an encapsulant because it offers a lot of advantages over other encapsulants. During the encapsulation process, another thing to consider is the dispensing inlet speed. The inlet speed will varying in this research to look at the effect on the pressure into the wire bond and identify the volume of fluid during the encapsulation process. The maximum pressure depends on the inlet velocity where the increase of inlet velocity, will be resulted in a decrease of pressure. Also, the greater inlet velocity shows a lower volume of fluid. ANSYS Fluent will be utilized to perform the encapsulation process virtually by utilizing VOF to stimulate the dispensing of EMC. An experiment was carried out to verify the theoretical result with experiment results.

CHAPTER 1

INTRODUCTION

1.1 Overview

In modern manufacturing, Light-emitting diodes or also known as LED light is widely used in industries for emits light to brighten up the space. LED light is currently the most energy-efficient lighting technology available for commercial and business applications, since it promises to be over ten times more efficient than incandescent light (Shine Retrofit, 2014b)

In the end of the 18th century, oil lamp was first invented for illumination purposes. Before that, human simply structured the hollow rock which holds a piece of moss soaked in animal fat that burns with a flame. Human also used other material for a body of the lamp which are terracotta, marble and metal and instead of fat, oil was used such as fish and olive oil. Wick was also often added to prolong burning of the flame (History of Lamps, 2020).

In the early 19th century, kerosene lamps were adopted in Germany once new energy sources were established. It was a kerosene-filled container into which a wick or mantle was dipped and burned. A glass chimney or a globe protected the flame from a draft in the container (History of Lamps, 2020).

Thomas Edison patented the incandescent light bulb in 1879, and a year later he began commercialising it. The first steady electric light was exhibited in 1835, and for the next 40 years, scientists all over the world experimented with the filament and the bulb's environment. These early bulbs had extremely limited lifespans, were prohibitively expensive to manufacture, and consumed excessive amounts of energy (Rebecca Matulka & Daniel Wood, 2013).

George Inman headed a team of General Electric scientists in the development of a more practical fluorescent lamp. In 1938, the team created the first practical and viable fluorescent lamp, which was sold for the first time.

Experiments in the 1950s with the semiconductor Gallium Arsenide finally led to the creation of the first working LED. In 1962, Nick Holonyak Jr. invented the

first LED that could produce visible red light. He designed these red diodes while working for General Electric (Shine Retrofit, 2014a).

Light-emitting Diode (LED) take over the traditional lamp such as incandescent light and fluorescent light as it has a lot of advantages over all the traditional lights. LED light has a lifespan 4 times better than fluorescent light and 40 times better than average incandescent light. It also promising the high efficiency as it consumes very low amounts of power. LED light also have a great Color Rendering Index (CPI) as it produces natural light emission that make the space more visible. This type of light also suitable for the usage in the illumination purposes as it consider as environmentally safe as it not contains mercury inside the bulb.(Stouch Lighting Staff, 2020)

1.2 Project Background

To put it simply, a light-emitting diode (LED) is a semiconductor device that emits light when an electric current is passed through it. When the current-carrying particles, known as electrons and holes, combine within the semiconductor material, light is created. LEDs are solid-state devices because light is created within the solid semiconductor material. The name "solid-state lighting," which includes organic LEDs (OLEDs), distinguishes this type of lighting from others that employ heated filaments (incandescent and tungsten halogen lamps) or gas discharge (fluorescent lamps) (LEDs Magazine, 2004).

Light-emitting Diode (LED) take over the traditional lamp such as incandescent light and fluorescent light as it has a lot of advantages over all the traditional lights. Because of its high luminous efficiency, extended lifetime, high reliability, and energy-saving qualities, light-emitting diodes (LEDs) are widely utilised in lighting applications (Wang *et al.*, 2015). However, without effective thermal management, an LED's lifetime and performance might be severely reduced (Weng, 2009). In contrast to an incandescent bulk filament working at temperatures above 1000°C, LED junction temperatures should be kept below 125°C (Xiao *et al.*, 2017). Because of the heat generated by the chip and phosphor, roughly 60%-70% of the electrical power in standard LEDs is converted to heat dissipation, and even greater for phosphor-converted LEDs. The current demand for high-brightness LEDs

raises their power to more than 1 W, even up to 5 W, and an LED chip's heat flux can range from 100 W/cm2 to 500 W/cm2. A high chip junction temperature causes a considerable shift in the main luminescence wavelength, as well as a reduction in optical efficiency and lifetime (Arik, Petroski and Weaver, 2002). In general, a 10-15°C increase injunction temperature can cut longevity in half (Schmid *et al.*, 2017). Thermal concerns have arisen as a result of these phenomenon in the development and deployment of high-power LEDs.

Several studies have attempted to improve the cooling solutions for high power LEDs, recognising the relevance of thermal management. A few examples of the methods are forced air(Deng *et al.*, 2017), radial heat sink(Yu, Lee and Yook, 2011), piezoelectric fan(Açikalin *et al.*, 2004), liquid cooling(Lai *et al.*, 2009) and heat pipe(Lin *et al.*, 2011). Although, these methods can reduce to some extent the junction temperature of an LED chip, they also have intrinsic flaws for high-power LED such as low reliability, a convoluted construction, bulkiness, high cost, and coolant leakage (Deng and Liu, 2010). The thermoelectric cooler (TEC) is one of the most used ways in mainstream applications among these systems (He *et al.*, 2015) due to its numerous advantages such as compact size, friendly to the environment , temperature control capability and fast reaction (Manikandan, Kaushik and Yang, 2017).

Gold wire bonding connects the chip electrodes to the lead frame. Wire bonding should be done with extreme caution; otherwise, bonding failure may occur and cause bond pad cratering, peeling, or cracking beneath the bond pad. The wire bonding procedure depends on the electrode placement on the chip. Usually, gold or copper has been selected for the materials of the bonding wires (Zhang and Lee, 2012).For this analysis, gold wire is chosen to make the interconnection with the printed circuit board(PCB. This is due to the fact that heat, pressure, and ultrasonic energy can easily bond gold wire. Furthermore, gold wire's junction size, bond strength, and electrical and thermal conductivity make it ideal for LED applications (Luo and Hu, 2013).The typical range of gold wire diameter is about 15μm to 50μm.In our research, we choose 1.2 mils which is equivalent to 30.48μm for the diameter of gold wire.

In this research for the type of bonding, ball bonding is used during semiconductor fabrication to make interconnections between an integrated circuit and a light-emitting diode (LED). Ball bonding is considered a suitable method for gold and copper wire since it required heat, pressure and ultrasonic energy to form the bond. In addition, ball bonding is also suitable for making the interconnection for a small wire diameter (Toyozawa *et al.*, 1990).Other than ball bonding, there is other technique for the wire attachment such as wedge bonding. Wedge bonding is a type of wire bonding in which ultrasonic power and force are used to produce bonds. But for this research, this type of technique is not suitable as it restricted only for the large diameter of wire.

Light-emitting diode (LED) are often formed by using clear encapsulant. Chemical inertness, stiffness, high-temperature stability, high optical transparency, and a high refractive index are all requirements for the encapsulant material (Kim *et al.*, 1999).Thus, Epoxy Moulding Compound (EMC) will be used as it has excellent electrical and mechanical characteristics, as well as excellent chemical resistance and low viscosity. Because there is contact between these two components, the amount of Epoxy Moulding Compound (EMC) used during the encapsulating process may impact the gold wire (Tian *et al.*, 2011).

1.3 Problem Statement

Among the topics discussed in the previous research, there are very limited literature focusing on the effect of stress and deformation on the gold wire during encapsulation process. By undergoing the encapsulation process, the inlet velocity might lead to the failure of Light-emitting diode (LED) which is from the excessive stress applied on the gold wire. The inlet velocity also might affect the dispensing of Epoxy Molding Compound (EMC) during the encapsulation process of Light-emitting diode (LED). Thus, the inlet velocity will be the parameter to stimulate the effect of the EMC dispensing and stress applied on the gold wire in this study.

1.4 Objective

The aimed of the study to fulfill the following objectives:

1. To study the effect of inlet velocity to the LED encapsulation filling by using Computational Fluid Dynamic (CFD).
2. To analyse the pressure on the LED wire with different inlet velocity.
3. To validate the simulation data with experimental results

1.5 Scope of Work

The scope of work is works that will be conducted to achieve objectives. ANSYS Fluent software will be using to complete this research since this software is used to simulate computer models of structures, electronics, or machine components for analyzing strength, toughness, elasticity, temperature distribution, electromagnetism, fluid flow, and other attributes. Volume of Fluid (VOF) will be utilized as it considered as an effective simulation methodology for this research. Basically, the Volume of Fluid (VOF) approach is a numerical free-surface modelling tool for tracking and identifying the free surface. The data that obtained will be compared with the experimental results as the experiment will be conducted also for the data validation.

CHAPTER 2

LITERATURE REVIEW

Light-emitting diodes (LED) are widely employed due to their superior characteristic over traditional light sources such as high luminous efficiency, high durability, prolonged lifetime, and low- power consumption. A bare LED chip may light up, but it cannot be used because of its low long-term dependability.

LED chip packing not only improves the stability and optical qualities of LED devices, but it also allows for control and adjustment of the final performance. LED chip packing is a need for LED use and has a significant impact on the final optical and thermal performance of LED devices.

2.1 Geometry Modelling of Gold Wire in LED

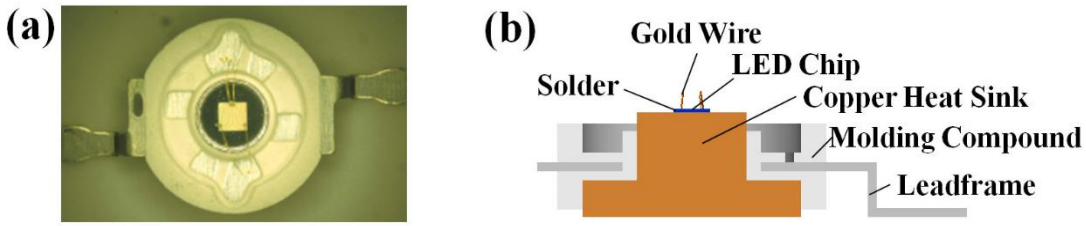

Figure 2.1 LED module without phosphor layer and encapsulates:

(a)Top view;(b) Sectional drawing.

In this literature review, Luo and Hu, (2013) began by outlining the functionality and the structure of nitride LED chip packaging .(Luo and Hu, 2013) illustrates the typical LED package without phosphor and encapsulates as in Figure 2.1. Connecting IC chip pads to the lead frame is commonly done with gold wire. Specifically, this LED package will be using in our study during encapsulation process. After the gold wire bonding, the phosphor gel is freely poured on the LED chip bonded around the substrate, as shown in Figure 2.2. The lens is set on the substrate once the phosphor gel has hardened, and silicone gel is injected inside, as shown in Figure 2.3.

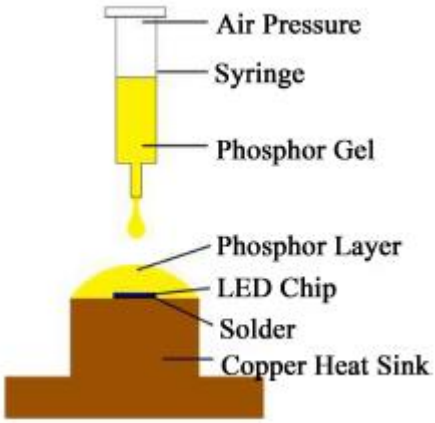

Figure 2.2 Freely dispersed phosphor coating process

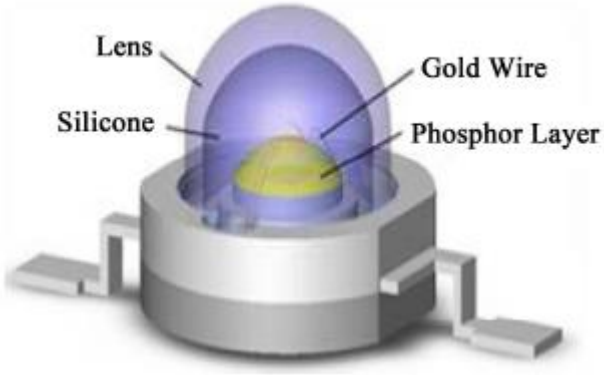

Figure 2.3 Typical 1W LED package

2.2 Effect of Wire Bonding on Optical Performance of LED Package

The aim of Wu *et al.*, (2012) study is to investigate the effect of gold wire shape and height on optical performance of LED package with freely dispersed phosphor layers. In ray tracing simulation software, four optical models of LED packages are constructed, and the simulation theory is based on the Monte Carlo approach. Figure 2.4 shows the structure of the LED optical model. During the construction of the optical model, some important simplifications are made.

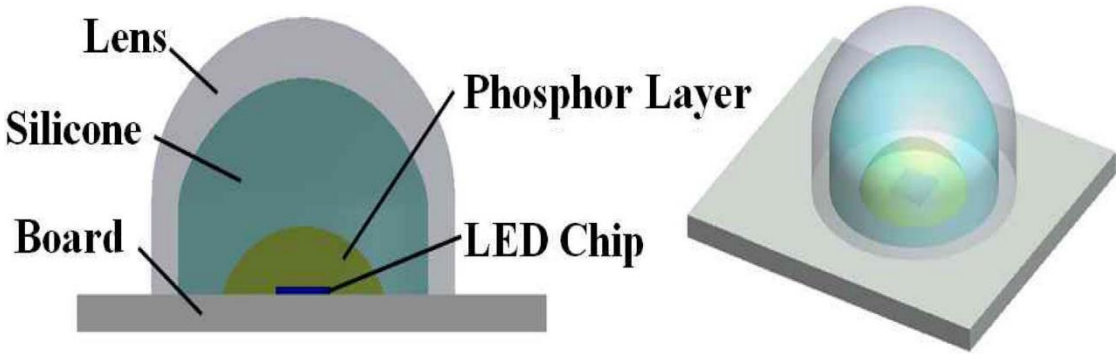

Figure 2.4 Schematic of optical model

Four sample of the optical model are labelled as samples 1 to 4. Figure 2.5 show the geometry of phosphor layer in sample 1 while Figure 2.6 show the phosphor layer in sample 2, sample 3 and sample 4 are corresponding to the ones with wire A, wire B and wire C(Wu *et al.*, 2012).

Figure 2.5 Front view and left view of phosphor layers in LED module without gold wires.

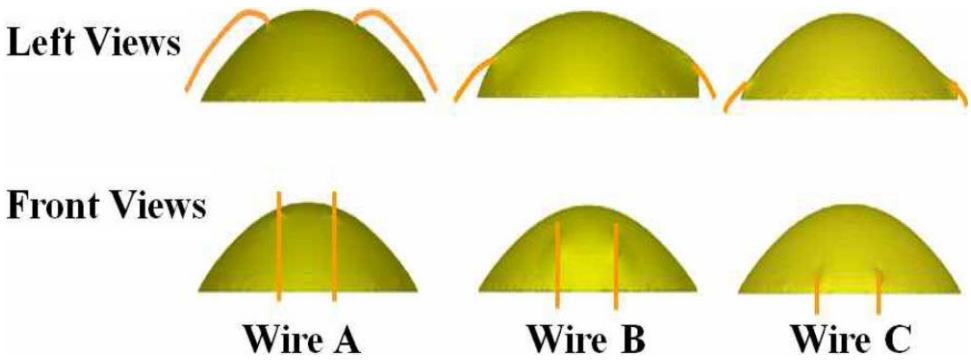

Figure 2.6 Phosphor profiles of three LED package samples.

Simulation results are shown in Figure 2.7. For all samples, the light intensity distribution (LID) is close to Lambertian. Lambertian refers to a surface that appears evenly bright from all directions of view which reflects the entire incident light. The most intense light is found in the centre, with a value of roughly 0. 075W. Every sample's LIDs in plane C 0° - 180° and plane C 90° -270° are nearly identical. It appears that the gold wires, which modify the geometry of the phosphor layer, have only a minor effect on the package's LIDs.

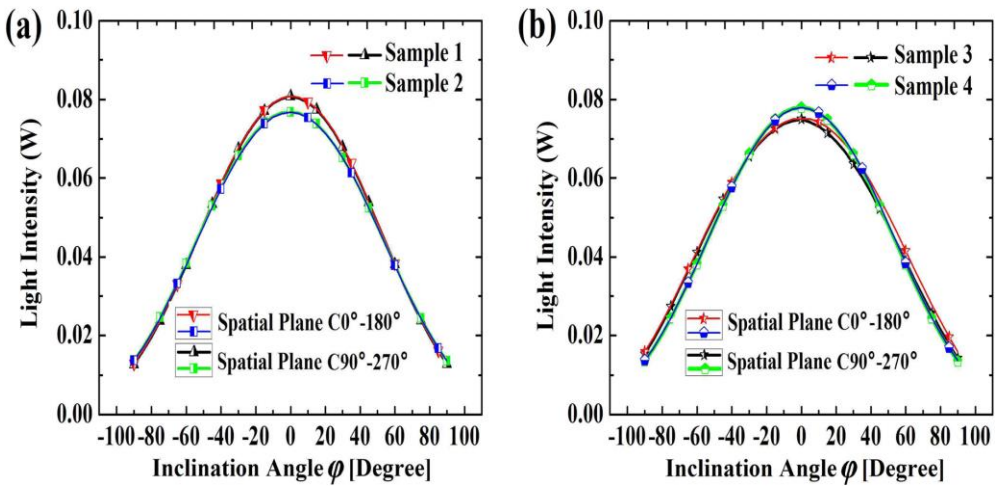

Figure 2.7 LIDs distributions at plane C 0° - 180° and plane C 90° -270 °

The yellow-blue ratio (YBR) is used in this study to show how angularly correlated color temperature varies (CCT). The larger the YBR, the lower the CCT. The smallest YBR is found in the centre, whereas it rapidly grows at the periphery, as illustrated in Figure 2.8. For sample 1, YBR increase considerably from 6.19 (at ϕ = 0°) to 13.37 (at ϕ = 90 °) at plane C90 ° - 270°. For sample 3 and sample 4, at ϕ = 0 °, YBR is 4.87 and 5.94, respectively. It is lower than the sample 1 value, indicating a larger angular CCT in the centre. That is due to the heights of phosphor layers are dragged down in LED packages with wire B and wire C, resulting in less blue light absorption and less re-emitted yellow light at the centre of phosphor layer.(Wu *et al.*, 2012)

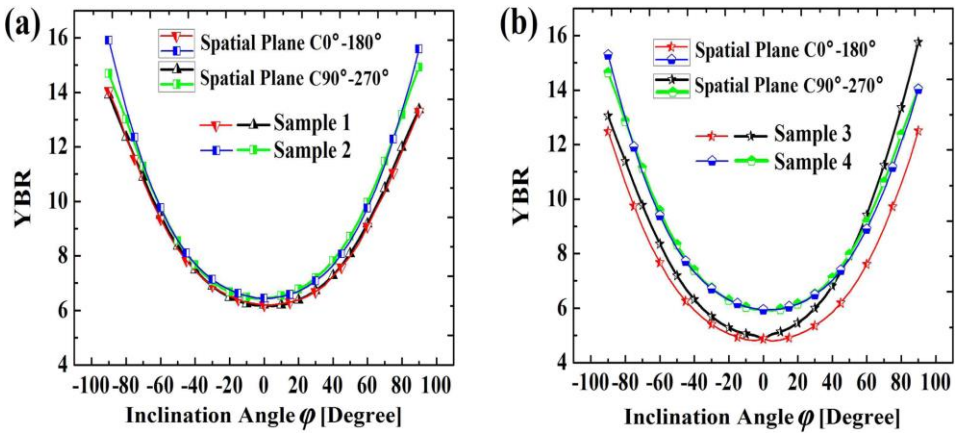

Figure 2.8 YBR distributions at plane C 0° - 180° and plane C 90° -270 °: (a)Sample 1, Sample2;(b) Sample 3, Sample 4.

As conclusion, wire B has the most negative impact on the shape of phosphor layer and its optical performance. Wire A has the least impact on LED packages when compared to the other two types of wire bonding. Wire C is not suitable for LED packing since it has a small impact. Because it is close to the top surface of copper heat sink, it is likely to cause a short circuit, which will harm the LED package. As a result, wire A would be the proper form of wire bonding to be used for LED packaging.

2.3 Wire Bonding Lifetime Model

The study from Sung-Uk Zhang& Bang Weon Lee(Zhang and Lee, 2014) show that wire neck breakage throughout the thermal shock test is one of the major failure modes for LED packages. This is due to the heat strains placed on the wire. Because the number of heat cycles to failure is fewer than 10,000 and the load frequency is less than 10 Hz, wire neck breakage is classified as low cycle fatigue. As a result, the Coffin-Manson fatigue law was used to simulate the wire bonding lifespan. The model is shown as follows:

$$N_f = a(\Delta\varepsilon_p)^b$$

where N_f is the mean number of cycles to failure, $\Delta\varepsilon_p$ is the increment of volume averaging accumulated plastic strain between the first thermal cycle to the second thermal cycle. During the production process, the assumption has been made that residual stresses inside the wire could be ignored. Constant a and b are linear regression coefficients that have been calibrated. Weibull analysis is used to examine N_f, which is based on failure data from thermal shock tests. The finite element analysis matching to the given test conditions is used to calculate $\Delta\varepsilon_p$ (Zhang and Lee, 2014).

The wire neck snapped during the thermal shock test. The failure was discovered using the on-off test as well as the Non-Destructive Test (NDT). Minitab was used to explore and analyze the failures of all data points. The test data point is marked as DP in Table 2.1 (Zhang and Lee, 2014).

Table 2.1 LED package and test condition for thermal shock tests.

Number of DP	Size	Kind of silicone	Wire diameter (μm)	Wire height (μm)	Wire length (μm)	Wire loop
1	Large	A	25.0	190	1000	L1
2	Large	A	25.0	230	1000	L1
3	Large	A	25.0	190	1000	L2
4	Large	A	25.0	230	1000	L2
5	Small	B	30.0	200	650	L2
6	Small	B	30.0	300	650	L2
7	Small	B	30.0	200	920	L2
8	Small	B	30.0	300	920	L2
9	Medium	A	25.0	280	1100	L3

The number of cycles to failure, N_f, and the correlation coefficient for each data point are computed according to the analysis, as shown in Table 2.2. For linear regression, DP2, DP3, DP5, and DP8 are employed, with correlation coefficients greater than our threshold of 0.95 (Zhang and Lee, 2014).

Table 2.2 N_f and correlation for each data point

Data point	N_f	Correlation
1	215	0.897
2	254	0.981
3	131	0.959
4	166	0.931
5	1055	0.971
6	1227	0.946
7	819	0.943
8	604	0.969
9	813	0.921

Regression analysis might be performed using the numerical and experimental findings of the four design points that were chosen. The following are the wire bonding lifetime model coefficients:

$$N_f = 6.98(\Delta\varepsilon_p)^{-1.2}$$

The other results were utilized to compare with the lifetime model. The most significant difference is between DP6 and the wire bonding lifespan model. The lifetime model expected N_f to be 582 (Zhang and Lee, 2014).

According to the other research by Zhaohui Chen et al.(Chen, Liu and Liu, 2011) ,the deformed shapes and von Mises stress evolutions at different times during the whole wire bonding process are shown in Figure 2.9. With the capillary travelling down at the impact stage, the von Mises stresses of the bonding system increase. At the ultrasonic frequency, the von Mises stress distributions in the electrode structure develop on a regular basis.

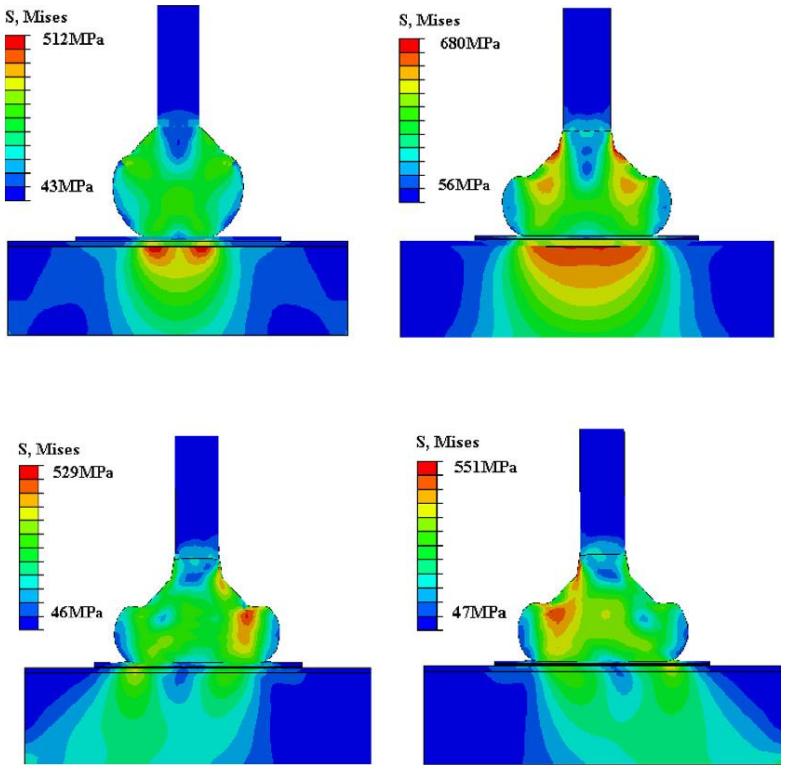

Figure 2.9 Deformed shapes and von Mises stress evolutions at different times during the wire bonding process.

Conclusion has been made from the data in Figure 2.9 which a greater friction coefficient causes a bigger plastic strain in the bond pad, which is beneficial for wire bonding quality but causes more stress in the ohmic contact layer beneath the bond pad. Finally, during the wire bonding process, the bonding force should be carefully monitored since it has a substantial impact on the stress and strain levels in the bond pad and ohmic contact layers beneath the bond pad.

Another approach was introduced by Yi-Cheng Hsu et al.(Hsu *et al.*, 2008) during the aging test to check the failure mechanism of high-power LED modules related with lens shape. Table 2.3 shows the relative output power of different types of LED modules with and without lenses. Due to greater heat dissipation, high-power LED modules enclosed with hemispherical-shaped plastic lenses had a longer lifetime than cylindrical-shaped and elliptical-shaped plastic lenses.

Table 2.3 Relative output power with lens and without lens for different types of LED modules

80℃	Relative output power (%)		
Structure	Type I (181 days)	Type II (181 days)	Type III (127 days)
With lens	44.6	13.8	15.8
After removing lens	52.7	70.8	36.6
Percentage increased after removing lens	8.1	57.0	20.8

According to the findings, the optical power of these high-power LED modules increased after the plastic lens was removed because the lens material degradation reduced the amount of light emitted to the front of the LED module.

As summary, many researchers had done their research to find the limitation or lifetime of the wire bonding by undergoing a few tests such as thermal shock test and aging test. The previous study can be related with this research as the research has a connection between it. Thus, the deduction has been made that the LED chip packaging is important to determine the final optical and thermal performance of LED devices.

2.4 Contribution of the Study

From the literature review studied,(Luo and Hu, 2013) describe the functionality and structure of nitride LED chip packaging. The structure of LED chip packaging can be used in this study as the type of LED chip packaging was similar. Also, the type of wire bond used in (Luo and Hu, 2013) study was a typical wire bond which is gold wire. This study can be related with this current study which used the typical LED package.

The other research that be related with this study was wire bonding lifetime model study by (Zhang and Lee, 2014).This study explains wire neck breakage of gold wire during the thermal shock test due to the heat strains. The test conducted can classified and selected the best wire bond to be used in this study which simulated the encapsulation process of LED.

As conclusion, the previous research has been done to study the wire bonding process and the test conducted for testing the bond wire during the encapsulation process. Thus, the previous study can be related with this current study.

CHAPTER 3

METHODOLOGY

3.1 Work Flow Chart

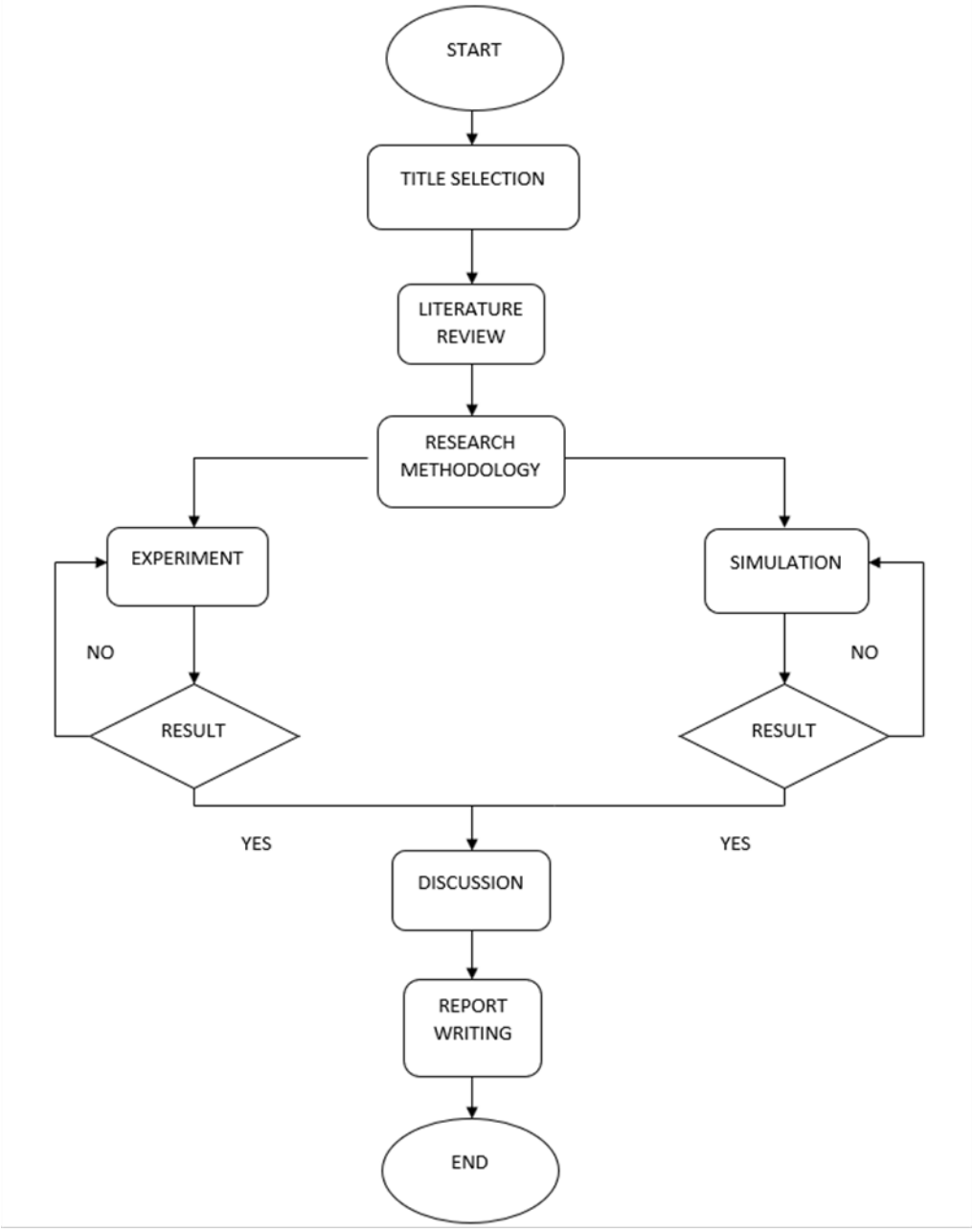

Figure 3.1 Workflow Chart

The workflow chart illustrated as in Figure 3.1. The study started with selection of title and writing on literature review. Literature review writing based on the previous study has been done. Then, the simulation conducted to obtain the result of LED encapsulation filling with different inlet velocity and effect of pressure to the LED wire. Moreover, the experiment was conducted to verify with the simulation result. Then, the results were compared in the report writing.

3.2 3D Incompressible Flow Equation

In this research, Computational Fluid Dynamics (CFD) has been used to analyse the LED encapsulation process which applied numerical analysis and data structure to solve the problem. Volume of Fluid (VOF) has been applied to analyse the dispensing of epoxy into LED and the interaction of gold wire with the epoxy during encapsulation process was conducted. By applying 3D incompressible flow equation such as continuity questionnaire-Stokes equation and conservation energy, we will be focusing on the dispensing process of epoxy.

The continuity equation as follows (Ku, Hirsh and Taylor, 1987):

$$\frac{\partial u}{\partial x} + \frac{\partial v}{\partial y} + \frac{\partial w}{\partial z} = 0,$$

where u, v,w are the velocity in x ,y and z direction.

The Navier -Stokes equation in the x,y and z direction as follows(Moser, Moin and Leonard, 1983):

$$\text{x: } \rho \left(\frac{\partial v_x}{\partial t} + v_x \frac{\partial v_x}{\partial x} + v_y \frac{\partial v_x}{\partial y} + v_z \frac{\partial v_x}{\partial z}\right) = - \frac{\partial p}{\partial x} + \mu \left(\frac{\partial^2 v_x}{\partial x^2} + \frac{\partial^2 v_x}{\partial y^2} + \frac{\partial^2 v_x}{\partial z^2}\right) + \rho g_x$$

$$\text{y: } \rho \left(\frac{\partial v_y}{\partial t} + v_x \frac{\partial v_y}{\partial x} + v_y \frac{\partial v_y}{\partial y} + v_z \frac{\partial v_y}{\partial z}\right) = - \frac{\partial p}{\partial x} + \mu \left(\frac{\partial^2 v_y}{\partial x^2} + \frac{\partial^2 v_y}{\partial y^2} + \frac{\partial^2 v_y}{\partial z^2}\right) + \rho g_y$$

$$\text{z: } \rho \left(\frac{\partial v_z}{\partial t} + v_x \frac{\partial v_z}{\partial x} + v_y \frac{\partial v_z}{\partial y} + v_z \frac{\partial v_z}{\partial z}\right) = - \frac{\partial p}{\partial x} + \mu \left(\frac{\partial^2 v_z}{\partial x^2} + \frac{\partial^2 v_z}{\partial y^2} + \frac{\partial^2 v_z}{\partial z^2}\right) + \rho g_z$$

where:

ρ =density

t=time

v=velocity

p=static pressure

μ=viscosity

g_x=gravitational acceleration

After the dispensing of epoxy completed, the interaction of the gold wire and the encapsulant will take placed and the pressure of the EMC to the gold wire will be analysed.

3.3 Simulation Setup

3.3.1 Modelling

By using Computational Fluid Dynamic (CFD) in Ansys Fluent, prediction of the flow of epoxy has been done during dispensing process onto LED and encapsulation process. The LED packages model was created as shown in Figure 3.2 by using Solidworks software.

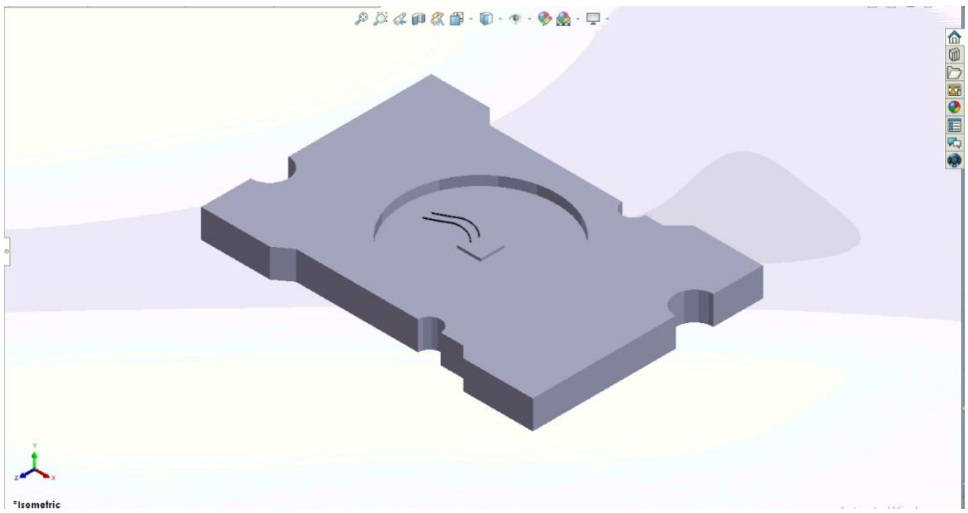

Figure 3.2 LED package with 2 gold wire attached.

Volume of Fluid (VOF) was used to record the flow of the epoxy during dispensing and encapsulation process. A 3D domain was created comprises needle head, air domain and LED substrate as shown in Figure 3.3 below. Figure 3.3 show the 3D domain while Figure 3.4 show the geometry of LED.

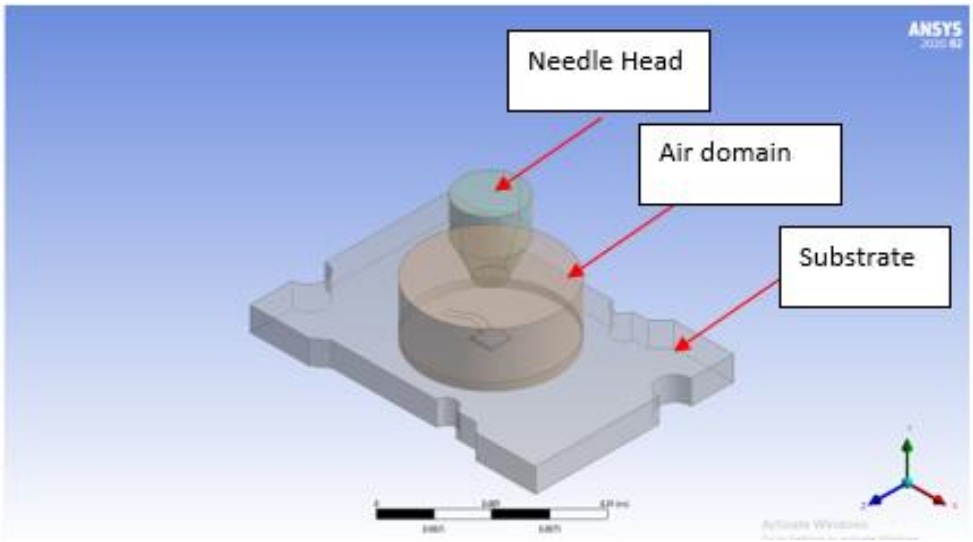

Figure 3.3 3D domain

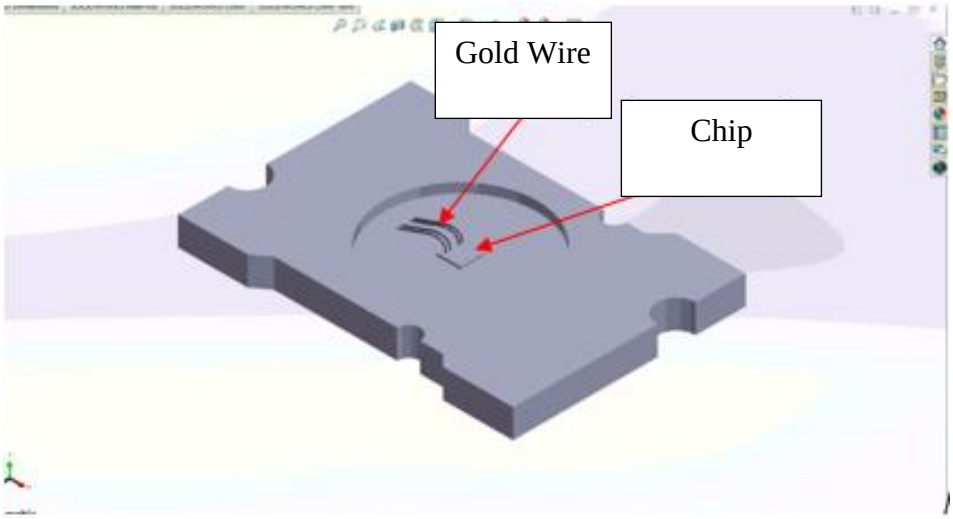

Figure 3.4 Geometry of LED

In this study, the simulation will be taken placed for 2 gold wire configuration which each of the gold wire was attached to positive and negative terminal, respectively. The configuration of gold wire should be precise to ensure the uniformity of the heat dissipated through the LED packages. The size of gold wire is approximately 0.03048mm respectively. The simulation will be analyse for 5 different inlet speed which is 1.58m/s, 2.58m/s, 3.58m/s,4.58m/s and 5.58m/s.

3.3.2 Meshing and Boundary Condition

All the bodies were meshed with structural elements consists of hexahedral and wedges for the air domain and needle head. Since the number of meshing elements is crucial in CFD simulation,5 different element sizes were examined. Mesh 1,2,3,4 and 5 represent the element size of 0.1 x 10^3m, 0.2 x 10^3m, 0.25 x 10^3m, 0.3 x 10^3 m and 0.5 x 10^3 m respectively. Figure 3.5 show the mesh quality for the 5 different types of element sizes.

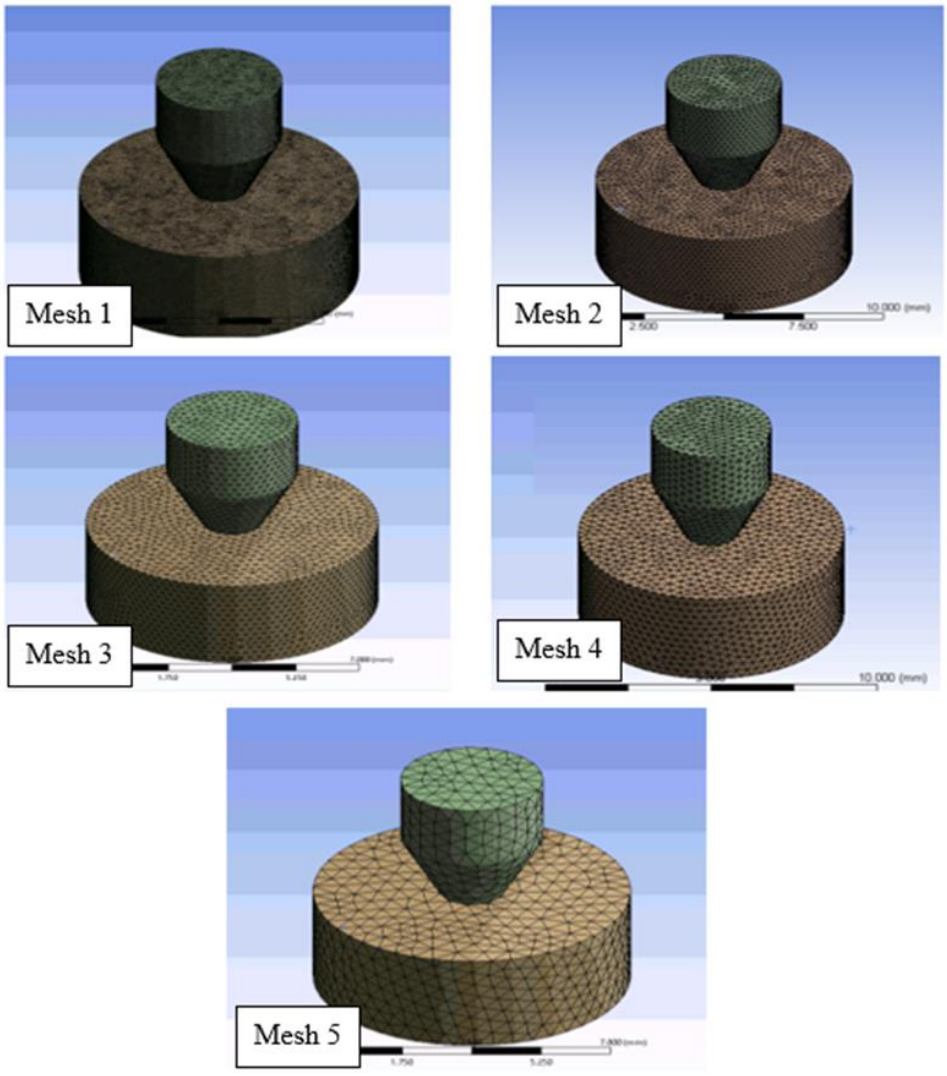

Figure 3.5 Mesh illustration for 5 different elements sizes

The aspect ratio for the meshing of the model also has been carry out to obtain the suitable mesh to be used in this simulation. The aspect ratio in meshing must not exceed 8 to obtain the suitable mesh. Figure 3.6 below show the aspect ratio of the respective mesh.

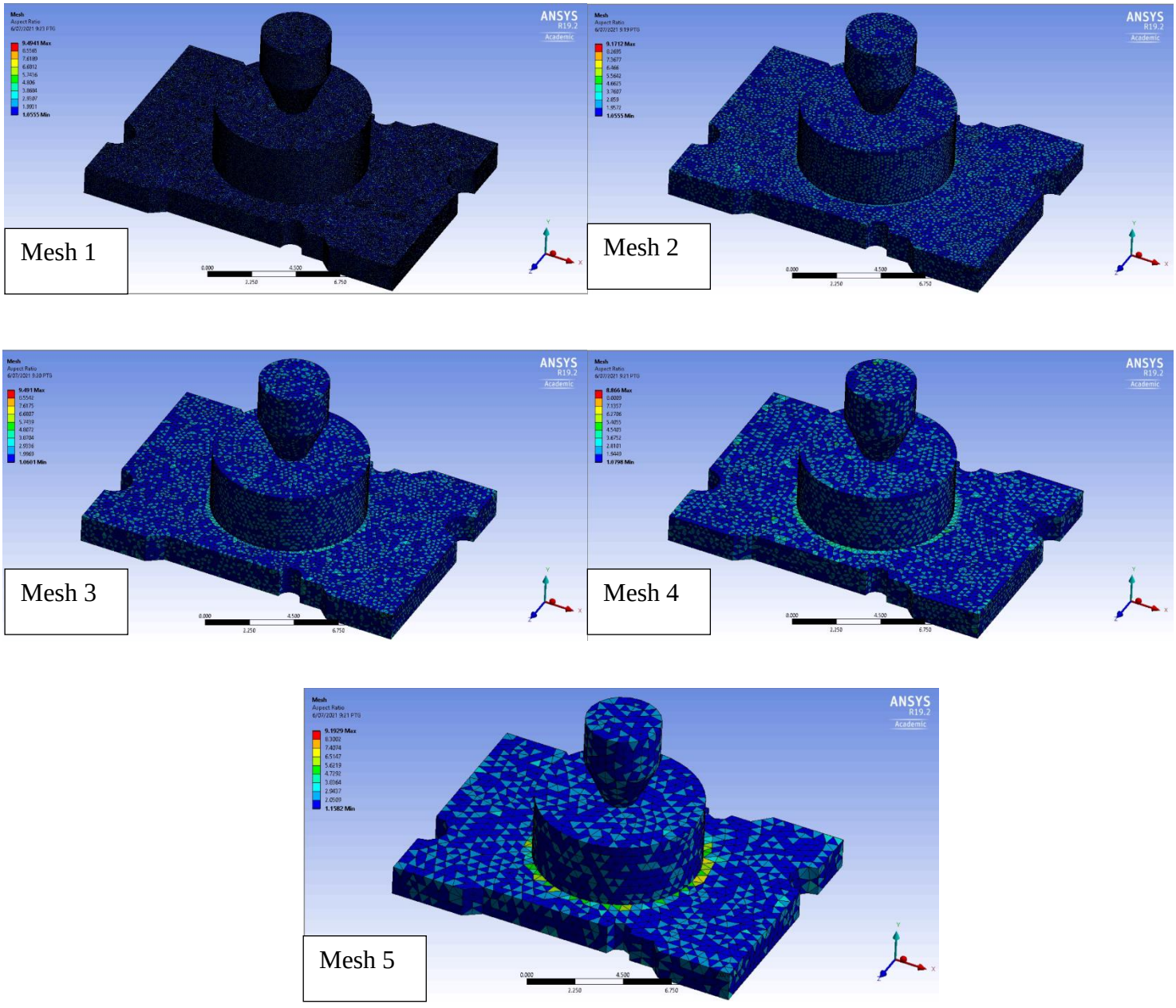

Figure 3.6 Aspect Ratio for the respective mesh.

Table 3.1 Aspect ratio value for respective mesh.

Mesh	Range of Aspect Ratio
Mesh 1	1.055-3.868
Mesh 2	1.055-4.663
Mesh 3	1.061-4.807
Mesh 4	1.079-5.405
Mesh 5	1.158-7.407

Based on Table 3.1, the range of aspect ratio for all types of mesh is not exceeding 8 which is suitable used in the simulation. To select the best mesh to be used in the simulation, Grid Independent Test will take place to ensure the suitable mesh to be used.

For the needle head body, the top surface was declared as inlet while the others declared as EMC wall. Meanwhile, for the air domain body, the top surface was defined as the outlet while the others declared as fluid wall. The interior of air domain or fluid is the zone where the EMC dispensed on the top of the substrate. The substrate wall and deforming wall also has been declared as shown in Figure 3.7.

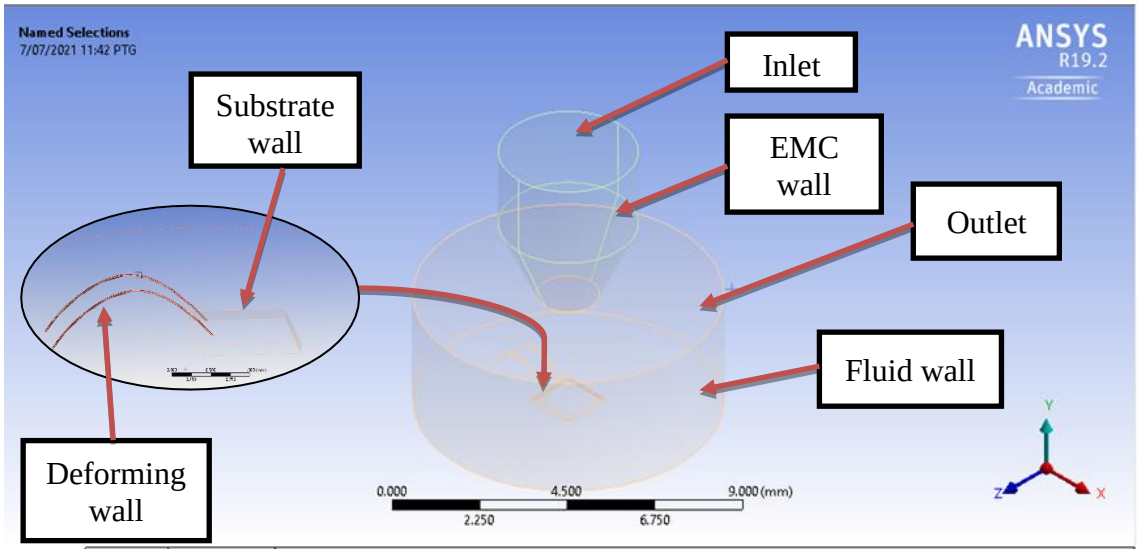

Figure 3.7 Boundary Condition

3.3.3 Material Selection and Volume of Fluid Setup

For this simulation, Epoxy Compound Molding (EMC) was selected as the fluid to be presence with the air. EMC is a non-Newtonian fluid with constant viscosity with zero shear stress. Moreover, density, viscosity and surface tension of EMC is shown as in the Table 3.2 while the properties of air are set to default.

Table 3.2 Material Properties

Properties	**Epoxy Molding Compound**
Density (kg/m^3)	1800
Viscosity (kg/m. s)	0.448
Surface Tension(N/m)	0.15

In this simulation, implicit multiphase VOF model was set. Laminar viscous model was used as the fluid flow of EMC. Then, the gravity was set in y-direction as -9.81m/s^2.Next , the materials used was defined based in parameter as in Table 3.1. The inlet contact angle was set to 135 °. The UDF was utilized to analyze the interaction between the EMC and gold wire with different inlet velocity was set. However, the injection time was fixed to 0. 010s.Furthermore, the time step size for this simulation was set to 1e-05s with 35000 number of time steps.

3.4 Experimental Setup

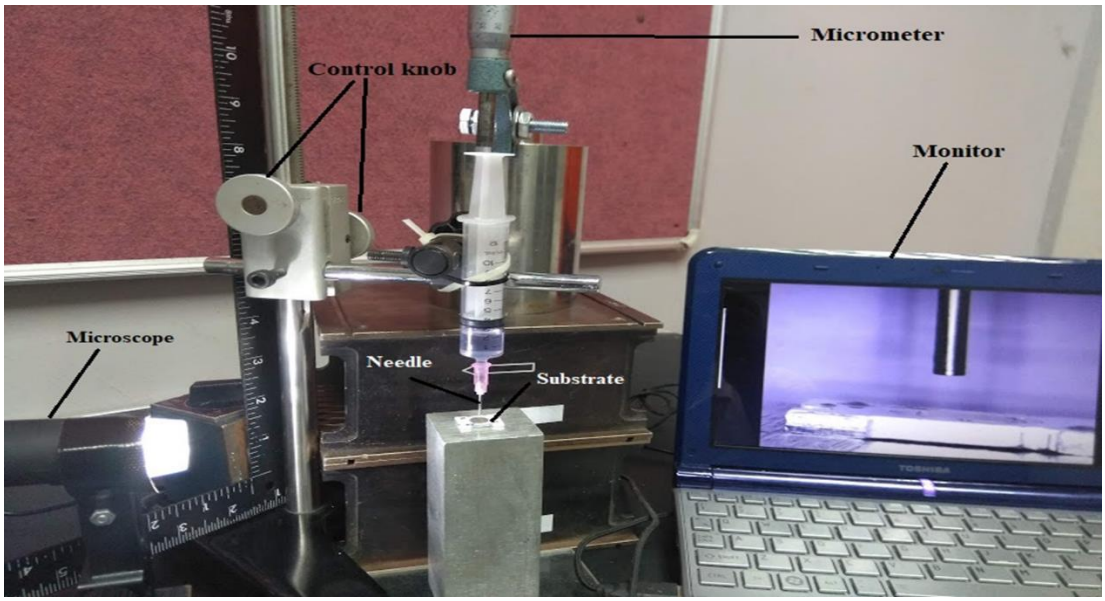

Figure 3.8 Setup of experiment.

In this study, the experiment will be conducted to validate the result with simulation data. Figure 3.8 show the experimental setup. This experiment conducted with different needle size which were 16G,18G,21G,22G and 23G.In this case, the experiment will be focused on 16G of needle size since 16G is the needle size used in simulation results. The inner diameter (ID) of 16G needle is 1.19mm and outer diameter (OD) is 1. 62mm.The needle length is approximately 12.5mm.

There are 3 methods to determine the density and droplet volume of epoxy which are measuring cylinder, open drop software and image system technique. Figure 3.9 show the measuring cylinder technique used in the experiment. For the measuring cylinder technique, the volume of epoxy obtained by measuring the number of droplets of epoxy per unit volume.